Preparation of Oriented Zeolite UTD-1 Membranes via Pulsed Laser Ablation

Trinidad Muñoz, Jr., and Kenneth J. Balkus, Jr.*

Contribution from the Department of Chemistry, University of Texas at Dallas, Richardson, Texas 75083-0688

Received July 22, 1998

Abstract: Thin films of the high silica zeolite UTD-1 have been prepared by using pulsed laser ablation onto polished silicon and for the first time on porous stainless steel disks. A post hydrothermal treatment of the laser deposited films in a UTD-1 synthesis gel results in oriented crystal growth. Densely packed planklike crystals of UTD-1 grow from the laser deposited film resulting in the ultra-large pores of UTD-1 oriented perpendicular to the support. The oriented UTD-1 membrane grown on porous stainless steel was evaluated for the room temperature separation of a *n*-heptane/toluene mixture, and selective permeation of the paraffin was observed.

Introduction

Nanoporous molecular sieves are attractive materials for membrane-based applications in part because of their selective adsorption properties imparted by their uniform pore structure. The utility of zeolites as membrane materials depends on the ability to prepare continuous defect free films. Depending on the type of zeolite, hydrothermal synthesis conditions, and in some cases the type of support, it is possible to obtain zeolite membranes having a particular orientation. Various techniques have been implemented in the fabrication of zeolite membranes. One approach has been the direct crystallization of zeolites such as ZSM-5 on supports in which a free-standing zeolite membrane can be removed from the substrate.[1] A problem with free-standing zeolite membranes as with most ceramic membranes is that they are generally quite fragile. This is further complicated by the fact that practical application of these microporous materials may require thin films. Therefore, most of the effort in this area has been in supported zeolite membranes.[1−13] Again the simplest strategy is to grow crystals onto a surface. A disadvantage with this approach is that isolated crystal growth can occur and as a result, the crystals must be grown large enough to form a continuous and defect-free film. Table 1 provides a representative list of zeolite membranes prepared by this method which are mostly small and medium pore size zeolites As can be seen from this table some zeolites have been prepared as oriented films. However, the control of the pore orientation in the membrane remains quite a challenge. Preferred crystal orientation offers several advantages in optimizing the efficiencies of gas separations as well as catalytic processes. Oriented zeolite membrane growth has been limited to those zeolites having MFI[1,2,12,14−29] and LTA[12,21] topologies.

We have reported a method for the preparation of molecular sieve thin films using pulsed laser ablation.[30−36] Recently, we obtained for the first time an oriented film of zeolite UTD-1 by

(1) Bein, T. *Chem. Mater*. **1996**, *8*, 1636.
(2) Geus, E. R.; den Exter, M. J.; van Bekkum, H. *J. Chem. Soc., Faraday Trans.***1992**, *88*, 3101.
(3) Sano, T.; Kiyozumi, Y.; Maeda, K.; Toba, M.; Niwa, S.; Mizukami, F. *J. Mater. Chem*. **1992**, *2*, 141.
(4) Tsikoyiannis, J. G.; Haag, W. O. *Zeolites* **1992**, *12*, 126.
(5) Jansen, J. C.; Nugroho, W.; van Bekkum, H. *Proceedings of the 9th International Zeolite Conference Montreal*; von Ballmoos, R., et al. Eds.; Butterworth-Heinemann: Boston, **1992**, 247.
(6) Sano, T.; Kiyozumi, Y.; Maeda, K.; Toba, M.; Niwa, S.; Mizukami, F. *Proceedings of the 9th International Zeolite Conference, Montreal*; von Ballmoos, R., et al. Eds.; Butterworth-Heinemann: Boston, 1992; p 239.
(7) Mintova, S.; Valtchev, V.; Engström, V.; Schoeman, B. J.; Sterte, J. *Micropor. Mater* **1997**, *11*, 149.
(8) Cheng, M.; Lin, L.; Yang, Y.; Yang, W.; Xu, Y.; Li, X. *Chin. Sci. Bull.* **1997**, *42*, 37.
(9) Cheng, M.; Lin, L.; Yang, W.; Yang, Y.; Xu, Y.; Li, X. *Stud. Surf. Sci. Catal*. **1997**, *105*, 2233.
(10) Boudreau, L. C.; Tsapatsis, M. *Chem. Mater*. **1997**, *9*, 1705.
(11) Koegler, J. H.; Arafat, A.; van Bekkum, H.; Jansen, J. C. *Stud. Surf. Sci. Catal*. **1997**, *105*, 2163.
(12) Sano, T.; Kiyozumi, Y.; Kawamura, M.; Mizukami, F.; Takaya, H.; Mouri, T.; Inaoka, W.; Toida, Y.; Watanabe, M.; Toyoda, K. *Zeolites* **1991**, *11*, 842.
(13) Jansen, J. C.; Kashchiev, D.; Erdem-Senatalar, A. *Stud. Surf. Sci. Catal*. **1994**, *85*, 215.
(14) Yan, Y.; Tsapatsis, M.; Gavalas, G. R.; Davis, M. E. *J. Chem. Soc., Chem. Commun*. **1995**, 227.
(15) Jansen, K. C.; Coker, E. N. *Curr. Opin. Solid State Mater. Sci*. **1996**, *1*, 65.
(16) Katsukaba, K.; Murata, A.; Kuroda, T.; Morooka, S. *J. Chem. Eng. Jpn*. **1997**, *30*, 72.
(17) Coronas, J.; Falconer, J. L.; Noble, R. D. *AIChE J*. **1997**, *43*, 1797.
(18) van de Graaf, J. M.; Kapteijin, F.; Moulijin, J. A. *Chem Ind*. **1998**, *71*, 543.
(19) Kolsch, P.; Noack, M.; Lieske, E.; Toussaint, P.; Caro, J. *Stud. Surf. Sci. Catal*. **1994**, *84*, 1075.
(20) Jia, M. D.; Chen, B.; Noble, R. D.; Falconer, J. L. *J. Membr. Sci*. **1994**, *90*, 1.
(21) Kondo, M.; Komori, M.; Kita, H.; Okamoto, K. *J. Membr. Sci*. **1994**, *133*, 133.
(22) Xu, W.; Dong, J.; Li, J.; Li, J.; Wu, F. *J. Chem. Soc., Chem. Commun*. **1990**, 755.
(23) Nishiyama, N.; Ueyama, K.; Matsukata, M. *J. Chem. Soc., Chem. Commun*. **1995**, 1967.
(24) Matsukata, M.; Nishiyama, N.; Ueyama, K. *J. Chem. Soc., Chem. Commun*. **1994**, 339.
(25) Nishiyama, N.; Ueyama, K.; Matsukata, M. *Micropor. Mater*. **1996**, *7*, 299.
(26) Matsukata, M.; Nishiyama, N.; Ueyama, K. *Stud. Surf. Sci. Catal*. **1994**, *84*, 1183.
(27) Nishiyama, N.; Matsufuji, T.; Ueyama, K.; Matsukata, M. *Micropor. Mater*. **1997**, *12*, 293.
(28) Nishiyama, N.; Ueyama, K.; Matsukata, M. *Ceram. Process*. **1997**, *43*, 2724.
(29) Nishiyama, N.; Ueyama, K.; Matsukata, M. *Stud. Surf. Sci. Catal*. **1997**, *105*, 2195.
(30) Balkus, K. J., Jr.; Muñoz, T., Jr.; Gimon-Kinsel, M. E. *Chem. Mater*. **1998**, *10*, 464.
(31) Balkus, K. J., Jr.; Riley, S. J.; Gnade, B. E *Mater. Res. Soc. Symp. Proc*. **1994**, *351*, 437.

10.1021/ja982599x CCC: $18.00
Published on Web 12/17/1998

Table 1. Supported Molecular Sieve Membranes

membrane	support	separations	ref
ZSM-5	cellulose, porous clay, porous alumina, porous glass	propane/propene, H_2/CH_4, butane/isobutane, hexane/2,2-dimethylbutane, ethanol/water, H_2/butane, H_2/isobutane	1, 2, 12, 14, 15, 16, 17, 18
Silicalite	cellulose, porous clay, porous alumina (oriented)	ethanol/water, heptane/toluene, methanol/MBTE, H_2/isobutane H_2/SF_6, H_2/CH_4, hexane/2,2-dimethylbutane	1, 19, 20
NaA	porous alumina	ethanol/water	12, 21
Ferrierite	porous alumina	benzene/*p*-xylene, cyclohexane/benzene	22−29
Analcime	porous alumina	benzene/*p*-xylene, cyclohexane/benzene	22−29
Mordenite	porous alumina	benzene/*p*-xylene, cyclohexane/benzene	22−29
UTD-1[a]	porous stainless steel (oriented)	heptane/toluene	this work

[a] Prepared by pulsed laser ablation.

Figure 1. Framework structure of UTD-1 (oxygen atoms omitted for clarity) calculated with use of the crystallographic data in ref 38.

this method.[36] In this process a high-intensity excimer laser beam strikes a pressed zeolite pellet that generates a plume comprised of fragments of the target that deposit on a temperature-controlled substrate. The application of a post hydrothermal treatment reorganizes the laser-deposited zeolite film. This method offers several advantages over direct synthesis methods, including the preparation of well-adhered continuous and sometimes oriented films with control of the film thickness over a range of a few hundred nanometers to several microns depending on the experimental parameters.

Zeolite UTD-1 shown in Figure 1 has a one-dimensional channel system where the pores are 10×7.5 Å[37−41] in diameter. As an ultra-large pore material, UTD-1 would be attractive for membrane-based gas separations and catalysis. However, the 1-D channel would require a preferred orientation of the crystals for any practical application of UTD-1. In this paper we describe further studies on the pulsed laser ablation of zeolite UTD-1. As part of this effort it was discovered that the $Cp^*_2Co^+$ template used to make UTD-1 functions as a UV adsorber that permits ablation of the silica based zeolite. This is an example of a phenomenon we refer to as guest-assisted laser ablation (GALA).[42] Both silica and porous stainless steel frits were studied as substrates for the pulsed laser deposited (PLD) films. Post hydrothermal treatment of the PLD films results in oriented film growth with the UTD-1 pores normal to the substrate surface. The UTD-1 membrane supported on the stainless steel frit was evaluated for the room temperature separation of a model mixture of *n*-heptane and toluene. It appears the selective permeation of the paraffin can be achieved by using UTD-1 membranes. The preparation and characterization of these membranes are described below.

Experimental Section

Materials. The all-silica UTD-1 zeolite was synthesized according to the published procedure[38−42] by first combining 0.058 g of NaOH (Fisher) in 13.5 mL of deionized H_2O with 2.0 mL of a 29% aqueous solution of bis(pentamethylcylopentadienyl)cobalt(III) hydroxide (Cp^*_2-CoOH). The template solution was then mixed with 0.82 g of fumed silica (Aldrich) and stirred at room temperature for 1 h. The pH of the synthesis gel should be between 11.2 and 11.5. Further adjustment of the gel pH may be made with dropwise addition of a 5 M NaOH solution if necessary. The final gel having a molar ratio of 0.05NaOH:$1.0SiO_2$:$0.13Cp^*_2CoOH$:$60H_2O$ was transferred to a Teflon lined stainless steel autoclave (Parr) and heated under static conditions for 2 days. The resulting yellow crystals were suction filtered, washed with deionized water, and dried in air at room temperature. The as-synthesized material was characterized by powder X-ray diffraction (XRD), FT-IR spectroscopy, and scanning electron microscopy (SEM). Powder XRD data were obtained by using a Scintag XDS 2000 X-ray diffractometer. FT-IR spectra were recorded on KBr pellets with use of a Nicolet Avatar spectrophotometer. The scanning electron micrographs (SEM) were taken on a Phillips XL 30 series. GC analysis was conducted on a Hewlett-Packard 5890 Series II capillary gas chromatograph with a stationary phase AT-1 GC column and a film thickness of 5 μm. Front face emission spectra were recorded from self-supporting pressed pellets ∼2.5 cm in diameter with a SPEX FLUOROLOG spectrophotometer.

Thin Film Preparation. Zeolite UTD-1 targets were prepared by pressing a pellet ∼2.5 cm in diameter that was then placed into a controlled atmosphere chamber positioned ∼2.5 cm above the substrate at an angle of ∼40°. A Lumonics HyperEX-400 excimer laser (248 nm, KrF*) was used to ablate the molecular sieve target which results in ejected particles that deposit on a temperature-controlled substrate.

(32) Balkus, K. J., Jr.; Sottile, L.; Riley, S. J.; Gnade, B. E. *Thin Solid Films* **1995**, *260*, 4.
(33) Sottile, L.; Balkus, K. J., Jr.; Riley, S. J.; Gnade, B. E. *Mater. Res. Soc. Symp. Proc.* **1994**, *351*, 263.
(34) Balkus, K. J., Jr.; Sottile, L. J.; Nguyen, H.; Riley, S. J.; Gnade, B. E. *Mater. Res. Soc. Symp. Proc.* **1995**, *371*, 33.
(35) Balkus, K. J., Jr.; Ball, L. J.; Gnade, B. E.; Anthony, J. M. *Chem. Mater.* **1997**, *9*, 380.
(36) Balkus, K. J., Jr.; Ball, L. J.; Gimon-Kinsel, M. E.; Anthony, J. M.; Gnade, B. E. *Sens. Actuators B* **1997**, *42*, 67.
(37) Freyhardt, C. C.; Tsapatsis, M.; Lobo, R. F.; Balkus, K. J., Jr.; Davis, M. E. *Nature* **1996**, *381*, 295.
(38) Lobo, R. F.; Tsapatsis, M.; Freyhardt, C. C.; Khodabandeh, S.; Wagner, P.; Chen, C. Y.; Balkus, K. J., Jr.; Zones, S. I.; Mark, M. E. *J. Am. Chem. Soc.* **1997**, *119*, 8474.
(39) Balkus, K. J., Jr.; Gabrielov, A. G.; Sandler, N. *Mater. Res. Soc. Symp. Proc.* **1995**, *368*, 369.
(40) Balkus, K. J., Jr.; Gabrielov, A. G.; Zones, S. I.; Chan, I. Y. *Chem. Ind.* **1996**, *69*, 77.
(41) Balkus, K. J., Jr.; Biscotto, M.; Gabrielov, A. G. *Stud. Surf. Sci. Catal.* **1997**, *105*, 415.
(42) Gimon-Kinsel, M. E.; Muñoz, T., Jr.; Ayala, A.; Balkus, K. J., Jr. Manuscript in preparation.

The laser energy in the range of 55 to 125 mJ/pulse was measured with a Scientech pyroelectric head (Model 380402). A computer-controlled rastering mirror (Oriel) was used to reflect the laser beam 90° and raster the beam across the target material over an area of 5 mm. A focusing lens was used to decrease the spot size of the laser beam to 0.001 cm^2. During an ablation experiment only fresh as-synthesized UTD-1 target surface was ablated by using a 14 ns pulse length with an energy output of 90−100 mJ/pulse and a repetition rate of 10 Hz. The substrates were polished silicon wafers (Texas Instruments, Inc.) and a porous 316 L stainless steel disk of dimensions 6 × 1.5 mm with a porosity of 0.5 μm (Mott Metalurgical, Inc). The substrate was heated to ∼160 °C and a background pressure of O_2 was maintained at 150 mTorr. The rate of UTD-1 deposition under these conditions was ∼130 nm/min.

Post Hydrothermal Treatment. Post hydrothermal treatment on the laser-deposited films was carried out by first preparing a UTD-1 synthesis gel as described above. The UTD-1 film on silicon was positioned in the reaction vessel tilted at an angle of approximately 60° with the laser-deposited film facing down as to minimize having material deposit from the gel onto the wafer. The UTD-1 coated stainless steel disk was placed in a Teflon holder with the clean side covered with Teflon tape to prevent material from depositing in the frit pores. The UTD-1 films were hydrothermally treated at 175 °C for 18, 24, and 72 h with a growth rate of ∼0.2 μm per hour. After hydrothermal treatment the films were washed with deionized water and air dried. It should be noted that without protecting the clean frit surface the pores will become clogged.

Membrane Separation. The porous stainless steel disk with the reorganized UTD-1 membrane was calcined at 550 °C for 6 h to decompose the organometallic template and then the membrane was carefully washed several times with concentrated HCl to remove the residual cobalt. The membrane with an effective disk area of 31.6 mm^2 was then mounted with epoxy (Devcon High strength 2-ton white epoxy) in a glass tube having a 10 mm diameter containing a course grade glass frit. The separation of heptane and toluene was conducted by placing a 1:1 mixture (v/v) in contact with the membrane at room temperature. The permeation side was kept at a constant partial vacuum of ∼30 μm. The permeate was collected in a liquid nitrogen cold trap and analyzed by GC.

Results and Discussion

Thin Film Preparation. We have previously reported the laser ablation of various aluminophosphate molecular sieves including $AlPO_4$ and MeAPO materials (where Me = Co, Fe, Mn, Mg, V) onto different substrates.[30,33−38] More recently we extended this method to silicate-based zeolites which turned out to have special requirements (vide infra). The high silica UTD-1 is of particular interest because of the ultra-large pores and good thermal stability. To laser ablate UTD-1, the zeolite must first be pressed into a free-standing pellet. This UTD-1 target is composed of planklike bundles of yellow crystals approximately 5 to 10 μm in length. Figure 2a,b shows scanning electron micrographs of the before and after the free-standing pellet of UTD-1 target, which reveals the aggregates of plank shaped crystals have been partially fragmented due to the pellet-making process. After the UTD-1 target is irradiated with the laser beam there is a clear transformation of the pellet surface to give a rough amorphous appearance as shown in Figure 2c. Pulsed laser ablation of the UTD-1 target with a laser energy of 100 mJ/pulse and a repetition rate of 10 Hz results in the generation of a bright blue plume. To deposit well-adhered UTD-1 material from this plume the substrate temperature, background pressure, and deposition time must be decreased from that used for the MeAPO systems we previously studied.[31−36] Using laser energies similar to that used to deposit the phosphate type molecular sieves results in comparatively faster deposition rates. Additionally, UTD-1 films are adhered with lower substrate temperatures (160 vs >250 °C). However, the background pressure should be <150 mTorr of O_2 to obtain well-adhered UTD-1 films,

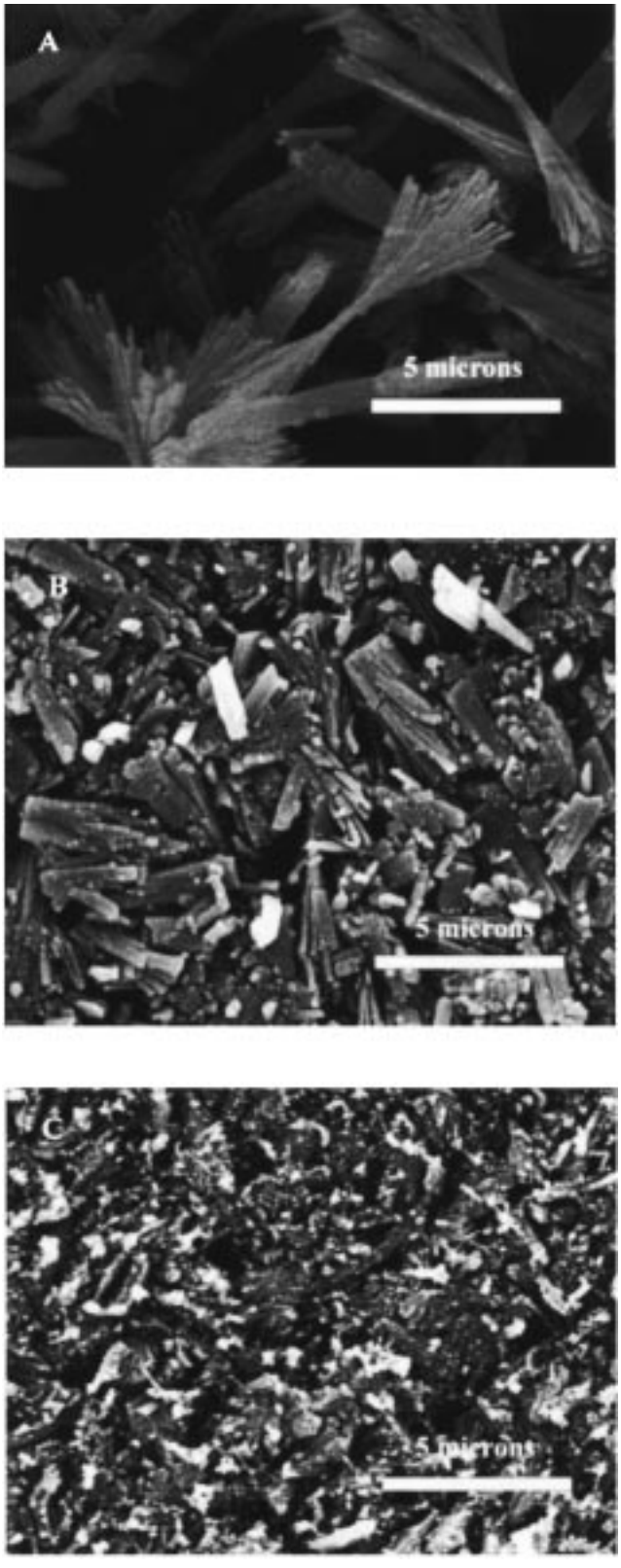

Figure 2. SEM of UTD-1 (A) as-synthesized bulk, (B) target pellet before ablation, and (C) target pellet after ablation.

which is lower than that for the aluminophosphates. This may suggest that the UTD-1 plume may be more sensitive to collisions with the background oxygen gas.

Figure 3a shows a SEM cross section view of a UTD-1 laser-deposited film on silicon that is approximately 700 nm thick. Upon close inspection of the laser-deposited film one finds that the film is composed of tightly packed nanoparticles derived

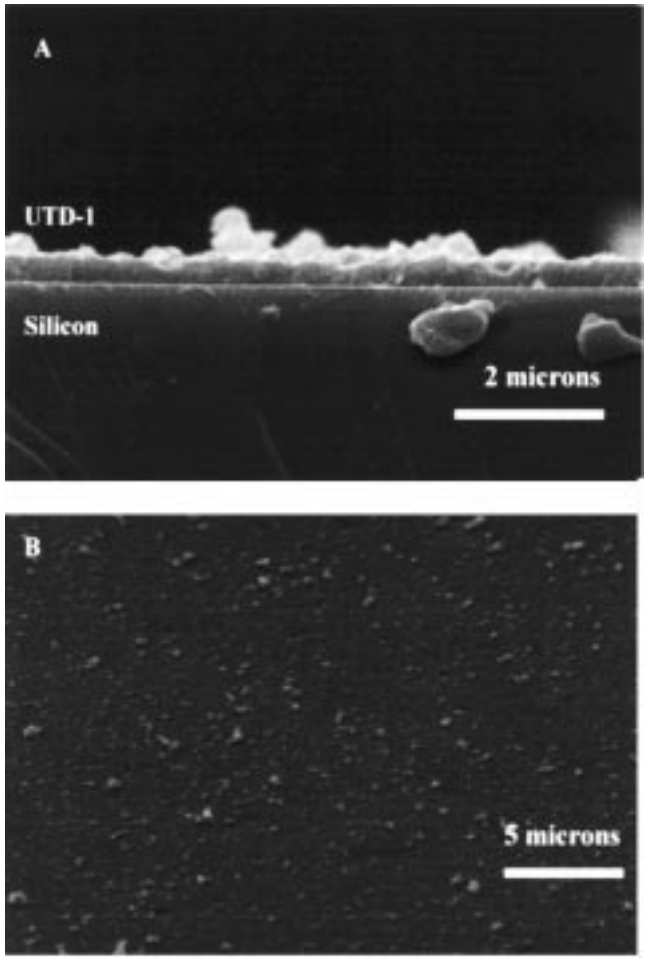

Figure 3. SEM cross-section view of (A) laser deposited UTD-1 on Si and (B) a surface view.

from the UTD-1 target. The surface of the deposited film appears rough and composed of small fragments of UTD-1 as shown in Figure 3b which arise from splashing.[43] The laser-deposited film appear largely amorphous by XRD. Figure 4 shows the FT-IR spectra of as-synthesized UTD-1 and a laser-deposited film on a KBr pellet. In the as-synthesized UTD-1 two strong bands at 1230 and 1091 cm^{-1} are the asymmetric stretches. The bands that appear at 809 and 780 cm^{-1} are assigned to the symmetric stretching modes while the more structure sensitive bands are in the region of 640−530 cm^{-1}. The band at around 460 cm^{-1} is assigned to the T−O bending mode. In the region of 2800−3000 cm^{-1} for as-synthesized and laser-deposited material there are bands at 2920 and 2855 cm^{-1} which are present in both materials and may be attributed to the C−H stretches associated with the methyl groups of the Cp* ring. In contrast, the laser-deposited film is missing the more structure sensitive bands consistent with the XRD. The main asymmetric band and the T−O bending band at 1038 and 440 cm^{-1} respectively have red shifted relative to the bulk UTD-1 material; however, the main asymmetric band in the ablated sample contains a shoulder at ∼1200 cm^{-1} that may be masking part of the asymmetric band present in the bulk UTD-1 material. In comparison with the amorphous silica used to make UTD-1, the main asymmetric band is present at ∼1100 cm^{-1}. Amorphous silica also contains a shoulder in the region of 800 and 950 cm^{-1}, which may be assigned to defect sites. It is evident that there are differences between the ablated UTD-1 and the

(43) Chrissey, D. B.; Hubler, G. K. *Pulsed Laser Deposition of Thin Films*; John Wiley and Sons: New York, 1994.

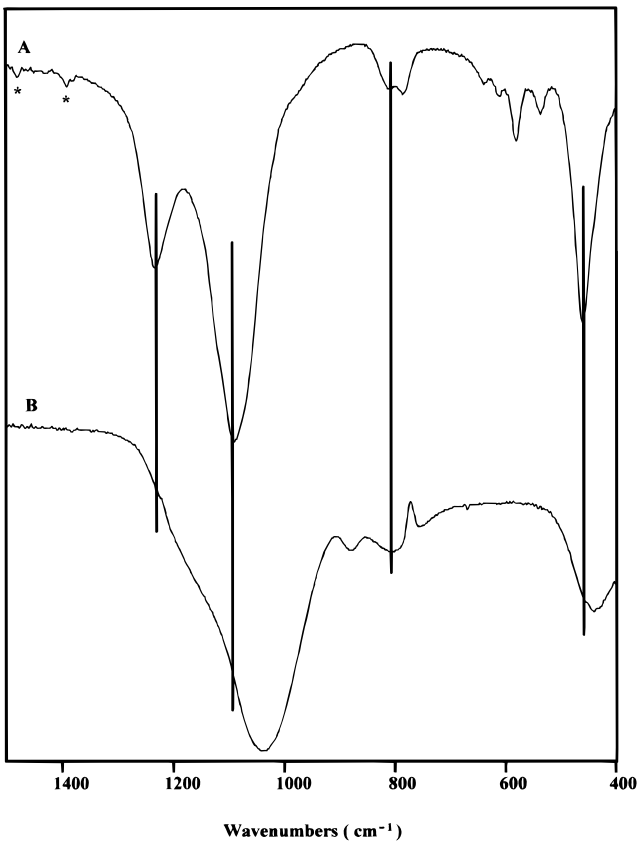

Figure 4. FT-IR spectra of (A) as-synthesized UTD-1 and (B) laser deposited UTD-1 (* denotes bands due to the template).

amorphous silica starting material which suggest there is no long-range order in the PLD films but there may be remanents of UTD-1 in an unknown form. Whatever the nature of these UTD-1 fragments they can be reorganized, thereby acting as seed layers or nucleation sites for recrystallization of the film. In the case of laser-ablated $AlPO_4$ and MeAPO materials, a post hydrothermal treatment in a synthesis gel or exposure to vapors of a template solution enhances the crystallinity of the PLD films.[34] Therefore UTD-1 films laser deposited on silicon were placed in a Teflon-lined Parr reactor containing a UTD-1 synthesis gel at 175 °C for 18, 24, and 72 h under static conditions. The silicon substrates were positioned in the autoclave at an angle of approximately 60° with the laser-deposited film facing down so as to avoid having UTD-1 material from the gel solution deposit directly onto the wafer. After an 18 h hydrothermal treatment, the coated substrate was removed from the reaction vessel and washed with deionized water. The SEM shown in Figure 5a reveals a fibrillar growth on the surface of the laser-deposited film. Powder X-ray diffraction shown in Figure 6b shows that crystalline material is beginning to form on the laser-deposited film having a thickness of ∼3.0 μm grown from the ∼700 nm thick PLD film. This is evident by the emergence of the 101 and 002 reflections of the UTD-1 molecular sieve. The gel mixture after 18 h is amorphous with no indication of solids in the reaction vessel. After 24 h, the SEM in Figure 5b reveals much less of the fibrillar growth and more of a continuous crystalline film with a thickness of ∼5 μm. Planklike crystals begin to form, which is typical of the bulk UTD-1 crystals as well as what visually appears to be a preferred orientation with the planklike crystals beginning to grow perpendicular to the substrate. The XRD pattern shown in Figure 6c reveals a fairly crystalline surface with increasing intensity of the of the 101, 002, 103, 301,

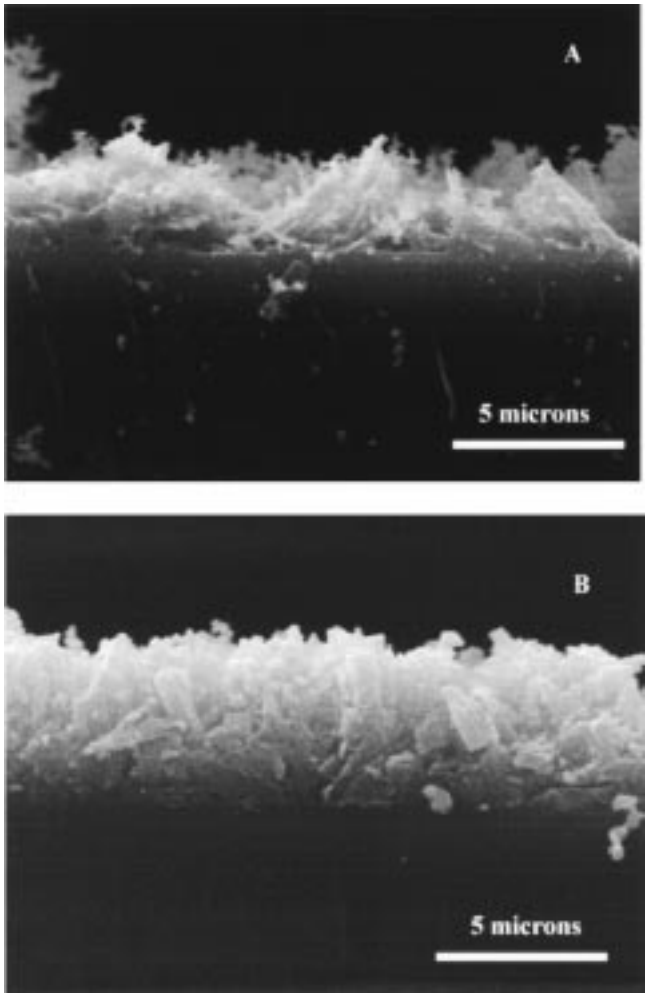

Figure 5. SEM cross-section view of a UTD-1 film (A) after post hydrothermal treatment in a UTD-1 synthesis gel for 18 h and (B) after post hydrothermal treatment in a UTD-1 synthesis gel for 24 h.

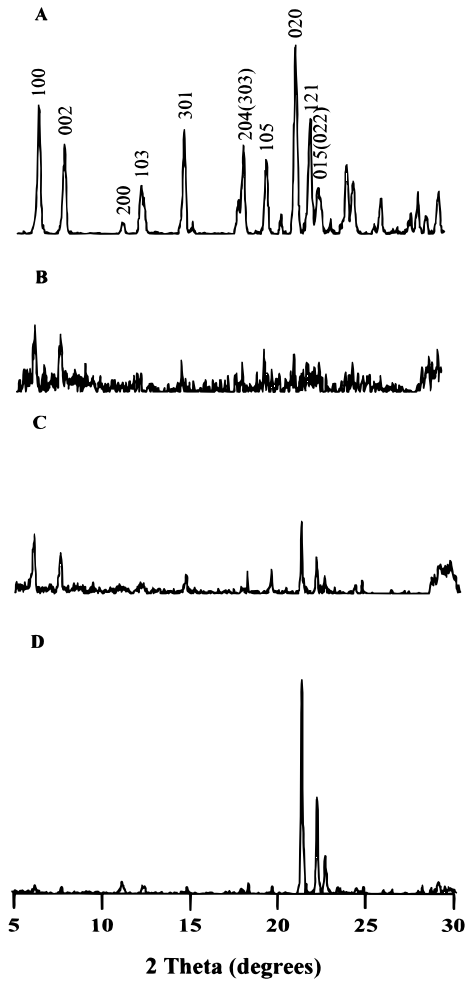

Figure 6. X-ray diffraction patterns of UTD-1 (A) as-synthesized bulk, (B) after 18 h of hydrothermal treatment, (C) after 24 h of hydrothermal treatment, and (D) after 72 h of hydrothermal treatment.

204(303), 105, 121, and 015(022) reflections and a large intensity increase of the 020 reflection. This supports the beginnings of oriented crystal growth visually observed by SEM since there is an increase in the intensity of the 020, 121, and 015(022) reflections with little increase in the (*h*0*l*) angle reflections. In both the 18 and 24 h hydrothermal treatments there was no evidence of bulk UTD-1 formation since no solid material was observed in the reaction vessel, which supports reorganization of the laser-deposited film. After heating for 72 h in the gel a continuous UTD-1 film approximately 11 μm thick had grown from the laser-deposited film as shown in the SEM in Figure 7. The morphology of the film appeared to be similar to what is observed for bulk UTD-1 material, which is generally composed of planklike bundles of crystals. It appears from the SEM that the UTD-1 crystals radiate up from the laser-deposited film where the one-dimensional channels are oriented perpendicular to the substrate along the length of the *b*-axis of the crystals. After this time there are crystals in the bulk gel such that UTD-1 crystals are loosely deposited on the reverse side of the silicon wafer which easily flake off.

The preferred orientation of the UTD-1 film was surprising and was verified by powder X-ray diffraction. XRD patterns for as-synthesized UTD-1 and UTD-1 grown on a silicon wafer after hydrothermal treatment for 72 h are shown in Figure 6a,d and illustrate preferred crystal growth orientation on silicon. In a bulk as-synthesized UTD-1 sample the crystals are randomly oriented and one obtains a diffraction pattern having the intensity ratios in Figure 6a. If, however, a crystalline material has preferred orientation, one would expect the diffraction pattern shown in Figure 6d. The X-ray powder pattern from the UTD-1 film grown from the laser-deposited film in Figure 6d shows the (020) reflection has greatly increased in relative intensity while most of the (*h*0*l*) reflections have decreased in intensity. This is consistent with the preferred orientation of the crystals where the direction of the channels (*b*-axis) is mostly perpendicular to the substrate. This is a significant achievement in the growth of oriented molecular sieves and represents the first example of an oriented ultra large pore channel type zeolite film. We anticipate an oriented large pore zeolite film of this type will find many applications ranging from gas separations to catalysis.

During hydrothermal treatment of the laser-deposited UTD-1 the pH of the initial gel is high (~11.3), which results in some etching of the silicon substrate as shown in Figure 7a. However, the associated morphological changes on the dissolved silicon do not appear to influence the regrowth and orientation of the UTD-1 film. This was shown when a clean silicon wafer was placed in a UTD-1 synthesis gel and heated under the same conditions as above. Figure 8 shows the top view of the UTD-1 film coating the polished side of the blank silicon wafer. It is obvious that the crystals in Figure 8 are randomly oriented and the film itself is not well adhered and easily flakes off the substrate. The UTD-1 film grown from the laser-deposited surface, however, exhibits preferred orientation and is well adhered to the substrate. It could therefore be concluded that

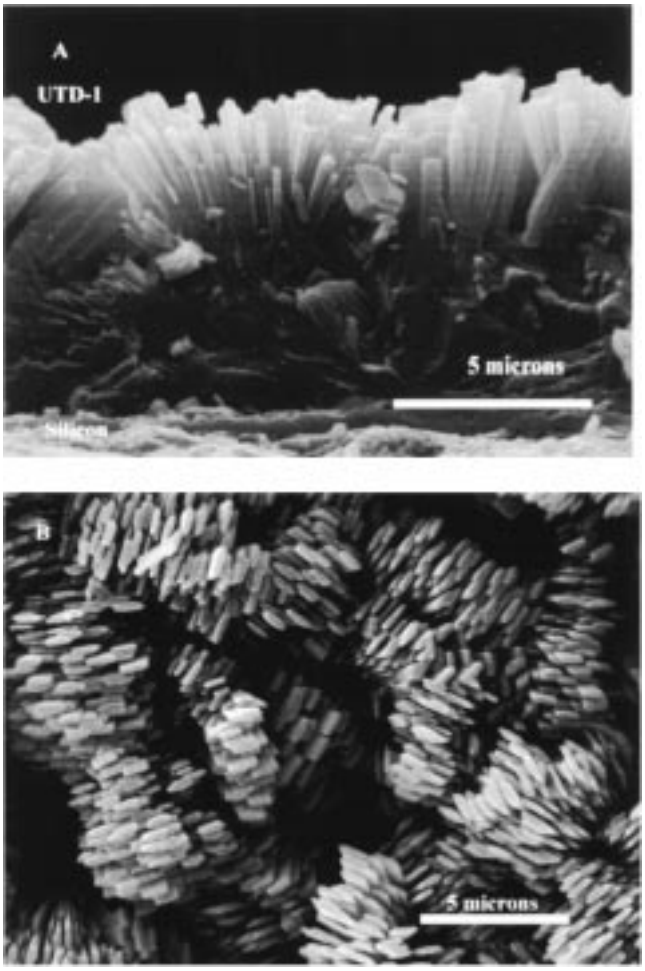

Figure 7. SEM cross-section view of a UTD-1 film (A) after hydrothermal treatment for 72 h and (B) a top view.

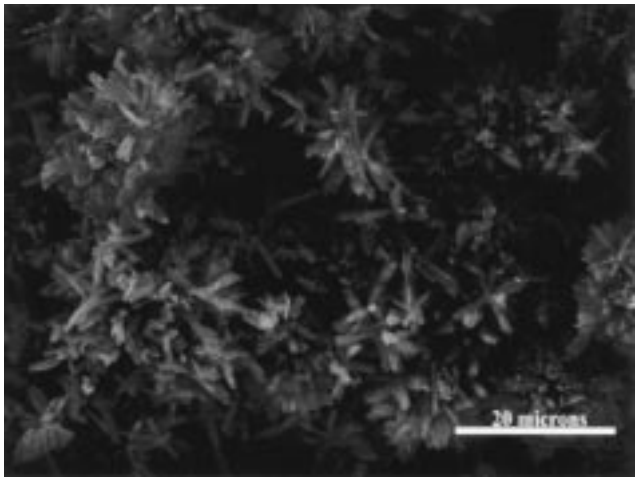

Figure 8. SEM of a UTD-1 film grown on a polished silicon wafer.

the laser-deposited surface is necessary to grow well-adhered and oriented UTD-1 films. One possible reason for this is that the laser-deposited UTD-1 film may provide nucleation sites which allow UTD-1 to grow quickly under hydrothermal treatment conditions. Generally, UTD-1 nucleates very slowly, i.e. there is no evidence of crystal growth up to 48 h of heating, whereas the PLD UTD-1 films exhibit crystallinity after heating for as little as 18 h with no evidence of crystal formation in the bulk gel even after 24 h.

The mechanism of the oriented zeolite crystal growth is not clear but there have been some efforts to improve our understanding of this process. For example, study on the surface crystallization of silicalite and ZSM-5 on different supports concluded that the adjustment of the synthesis conditions was shown to control the orientation of the crystals to a certain extent, such that for high concentrations a gel layer is formed at the substrate that regulates crystal growth and the resulting crystals are oriented parallel to the substrate. At low concentration of silica and at low temperature, the *c*-axis of the MFI crystals was shown to grow mostly normal to the support. This is the result of the low concentration of silica in the mixture which does not allow for the formation of a gel layer on the support. In our system, oriented crystal growth occurs not from a smooth clean surface but from a densely packed film on silicon composed of UTD-1 fragments deposited by pulsed laser ablation. These template-containing UTD-1 fragments may allow the surface to retain a memory effect and thereby provide seeds or nucleation sites for crystal growth to occur. It would seem that the PLD film is not preoriented since after 18 h of hydrothermal treatment the emerging crystalline film is not highly oriented. Even after 24 h a more crystalline and continuous film is formed, but the preferred orientation is only beginning to develop. The key to growing oriented PLD films may be with the crystal morphology where the planklike crystals having an aspect ratio of $b \gg a > c$ are generally observed. As the tightly packed PLD layer of UTD-1 fragments reorganize, the crystal growth takes the path of least resistance perpendicular to the substrate. Fortunately, this orients the channels normal to the surface. In contrast UTD-1 crystals deposited from solution on a clean surface grow randomly oriented because the nucleation sites are in solution not crowded on a PLD surface. The apparent increase in UTD-1 crystal orientation as the thickness increases is consistent with the idea that as the nuclei crystallizes, the forest of crystals thickens and upward growth is dictated. This phenomenon appears to be the opposite of other known oriented zeolite films where an initial seed layer deposited from solution is oriented by virtue of nanocrystal packing but subsequent crystal growth becomes random as the film thickness increases.[10]

The crystallization of UTD-1 requires the presence of the $Cp^*_2Co^+$ template. The organometallic is transferred to the substrate during laser ablation and must be partially occluded in the UTD-1 fragment. It was anticipated that the reorganization of PLD UTD-1 would require the presence of the structure directing agent in the film since previous work with phosphate-based molecular sieves demonstrated that the presence of the template was necessary to reorganize the PLD film to the same phase as the target.[33−38] In an effort to verify this for UTD-1 and further evaluate the role of the template in the reorganization step, a sample of UTD-1 was calcined to decompose the organometallic and then washed with HCl to remove the cobalt from the pores. Surprisingly, laser irradiation of a calcined UTD-1 sample resulted in no ablation of the zeolite target. Those areas of the calcined pellet that were laser irradiated showed a green luminescence when placed under a UV lamp. Figure 9 shows the luminescence spectrum of the laser-irradiated UTD-1 pellet acquired with a 350 nm excitation. The absorption of the excimer laser energy apparently produces defect sites in the molecular sieve. We have previously reported that excimer irradiation of all silica and aluminosilicate MCM-41 results in the generation of defect sites and associated luminescence.[44] This now appears to be a general phenomenon with the laser ablation of silicate-based materials. In the as-synthesized UTD-1 target the organometallic guest serves to absorb the UV excimer

(44) Gimon-Kinsel, M. E.; Groothius, K.; Balkus, K. J., Jr. *Micropor. Mesopor. Mater*. **1998**, *20*, 67.

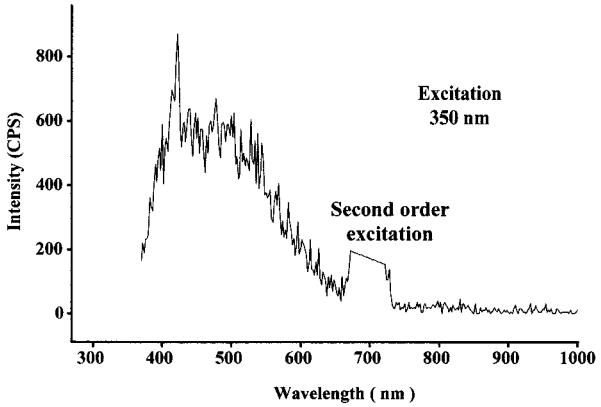

Figure 9. Photoluminescence spectrum of a laser irradiated UTD-1 target material.

irradiation and assist in the ablation of the molecular sieve material from the solid to the gas phase. We have also found that if the surfactant template is removed from MCM-41 and the UTD-1 organometallic template $Cp^*_2Co^+$ is exchanged into the mesopores, then pulsed laser deposition of MCM-41 was possible. We now refer to this phenomenon as guest-assisted laser ablation (GALA).[42]

An oriented large pore molecular sieve like UTD-1 would be an attractive material in the areas of gas separation and catalysis; however, for practical purposes, as seen from Table 1, the material would have to be placed on a porous support. As a result, UTD-1 was laser ablated onto a porous stainless steel support. Figure 10a shows an SEM of the stainless steel support before laser deposition of UTD-1 and Figure 10b shows an SEM of laser deposited UTD-1 on the porous stainless steel disk. Close inspection of this image reveals UTD-1 material coating the surface of the 500 nm pores with fragments of UTD-1 embedded in the channels and cavities of the support. The stainless steel disk was then subjected to a post hydrothermal treatment for 72 h. Again the SEM revealed a densely packed membrane of UTD-1 crystals growing perpendicular to the porous support. However, the orientation appears to be even more pronounced than on a silicon substrate. Figure 10c shows a top view of the porous support with sections of planklike UTD-1 crystals radiating upward and possibly mimicing the uneven topology of the stainless steel frit. Powder X-ray analysis of the membrane once again showed dramatic changes in the relative peak intensities. Figures 11a and 11b show the diffraction patterns of the bulk as-synthesized UTD-1 and a calcined UTD-1 membrane on porous stainless steel, respectively. Similar to the oriented film grown on silicon, the diffraction pattern of the membrane exhibits a large increase in relative intensity of the 020 reflection while most of the (*h*0*l*) reflections are depressed. Again this result is consistent with a preferred orientation of the crystals emanating from the laser-deposited surface where the direction of the channels (i.e. *b*-axis) is mostly perpendicular to the porous support. Figure 12a shows an SEM of oriented UTD-1 grown on a stainless steel support that has been cut away revealing a continuous film with a thickness of 14 μm and a top view of the membrane in Figure 12b. Close inspection of the film reveals that the crystals are mostly oriented perpendicular to the substrate from the top to the base of the membrane. For this oriented UTD-1 membrane to be useful, particularly in gas separations, it is necessary to remove the organometallic template occupying the pores. Calcination can pose a problem with supported membranes, for example, at temperatures up to 500 °C, which can cause thermal stress and lead to partial destruction of the membrane.[12] After calcination

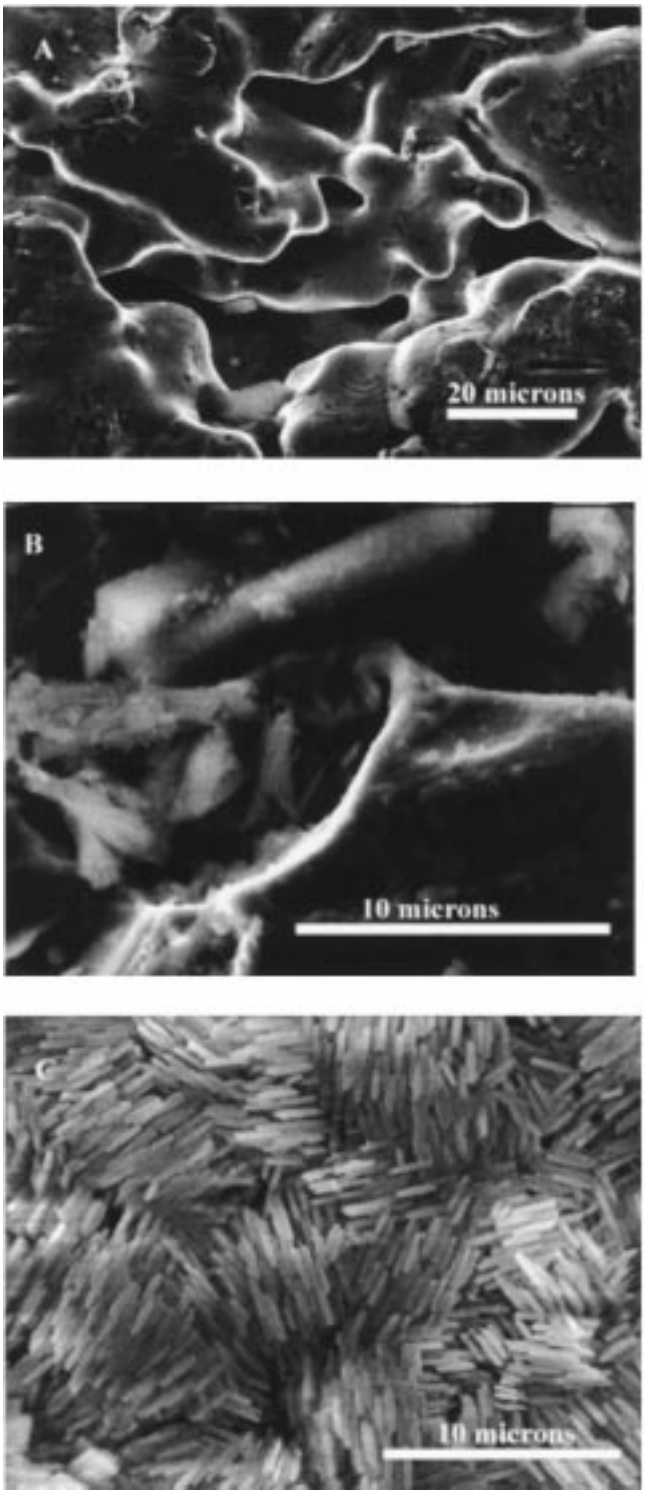

Figure 10. SEM of (A) stainless steel porous support, (B) laser deposited UTD-1 on the stainless steel porous support, and (C) an oriented UTD-1 membrane grown from a laser deposited film after a 72 h of hydrothermal treatment.

of the UTD-1 membrane on the porous support at 550 °C for 8 h, the powder XRD exhibited no decrease in crystallinity or preferred orientation. We can now test for cracks or defects generated by this treatment by attempting a model separation.

Membrane Separation. An attractive property of inorganic microporous membranes is selectivity; however, the diffusion through the micropores is a relatively slow process.[2] This means that very thin membranes are required for reasonable fluxes to be observed. The laser-ablation method readily allows for control

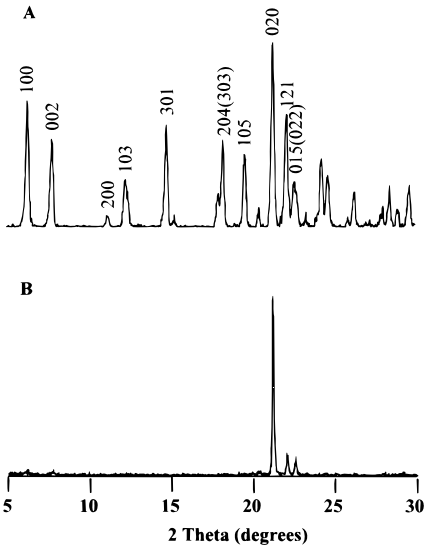

Figure 11. X-ray diffraction patterns of UTD-1 (A) as-synthesized bulk and (B) a calcined membrane on porous stainless steel.

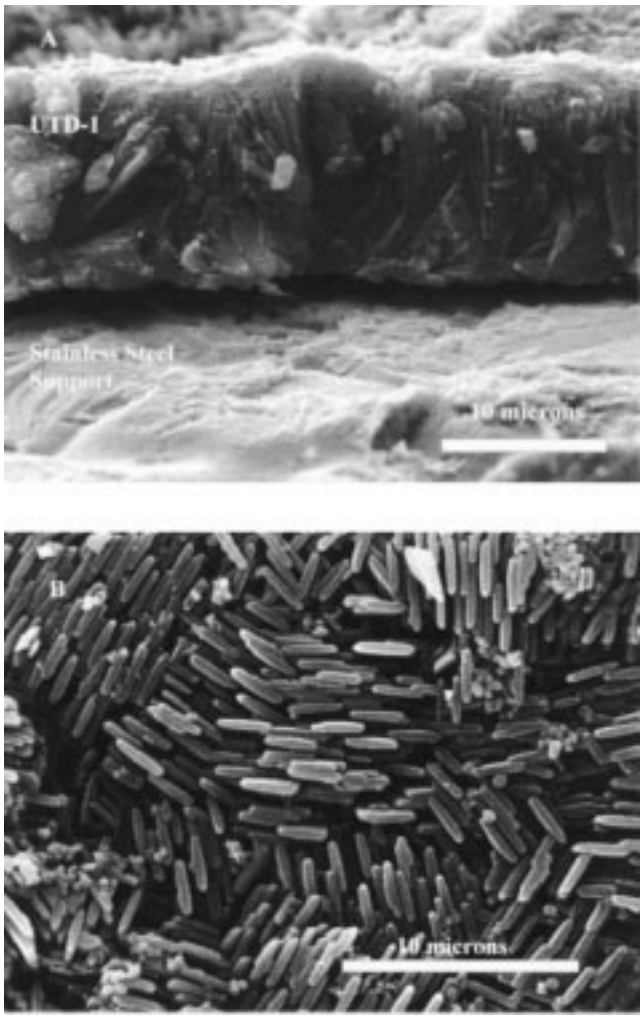

Figure 12. SEM cross-section view of a UTD-1 membrane (A) grown on a stainless steel porous support and (B) a top view of the UTD-1 membrane.

of deposit thickness, and submicron thick membranes should be easy to prepare. In the present study the UTD-1 membranes are probably more than an order of magnitude too thick to obtain useful fluxes. However, one goal with this preliminary experiment was to evaluate the selectivity for an important model separation. There is great interest in a membrane-based process for the separation of paraffin and aromatics generated in reforming reactions. One such application which requires the use of pure paraffins is the manufacture of detergents, in which paraffins serve as the alkyl constituent of sulfonated alkylaryl and alkyl sulfonate synthetic detergents.[45,46] Linear paraffins are preferred due to their superior detergent properties as well as better biodegradablility over synthetic detergents made with branched paraffins. Other important uses of linear paraffins are their use in flameproofing agents, solvents, and plasticizers.[45,46] Therefore as a model for this type of separation we selected a mixture of *n*-heptane and toluene. Preliminary separation experiments with a heptane/toluene (1:1, v/v) mixture were performed at room temperature with the feed in liquid form at atmosphere pressure while the down stream side was kept at a reduced pressure of ~30 mTorr. The permeated mixture was collected and sampled at different time intervals. The average mole percent of the heptane feed component was 38%. The mole percent of the heptane in the permeate collected at 3.5, 5.0, 7.0, and 14 h was 52%, showing an enrichment of the paraffin over the aromatic by a factor of ~1.5. One would not expect exclusion of one of these components based on size or shape because of the extra large pores; however, the differing affinities of molecules with the pore openings may play a role in separation.[27] Zeolites that have been employed in adsorption-type separations of paraffins and aromatics such as X- and Y-type zeolites also favor the paraffin over aromatics. One might take a lesson from zeolite-based adsorption processes for this type of separation and improve the selectivity by altering the UTD-1 framework composition. Additionally there are a host of other commercially relevant separations to be tested with the UTD-1 membranes.

Conclusions

Oriented extra-large-pore UTD-1 molecular sieves have been grown on flat silicon supports as well as porous stainless steel supports for the first time, which suggests that other substrates may also be possible. An important feature in the growth of these membranes appears to be the presence of a laser-deposited film on the substrate despite the fact that the film is X-ray amorphous. The laser-deposited film, however, can act as a seed layer or nucleation site for the recrystallization of the film. Furthermore, because the laser-deposited film is composed of tightly packed nanoparticles we propose that during post hydrothermal treatment, the recrystallization and further growth of the crystals along the long axis (*b*-axis) is restricted by the tight packing. As a result, the crystals are directed to grow perpendicular to the support. Now that we have prepared the first-oriented, extra-large-pore molecular sieve on a porous support, we can begin to explore the applications of these membranes in other types of separations, catalysis, and as chemical sensors. Furthermore, with the discovery that laser ablation of UTD-1 and MCM-41 requires the presence of an organometallic guest molecule (GALA), we can now generate thin films of virtually any molecular sieve.

Acknowledgment. We thank the National Science Foundation and the Texas Advanced Technology Program for financial support of this research. We also thank Dr. Mary Gimon-Kinsel for assistance with this project.

JA982599X

(45) Plee, D. U.S. Patent 5,731,488, 1996.
(46) Schreiner, J. L.; Britton, R. A.; Dickson, C. T.; Pehler, F. A., Jr. U.S. Patent 5,220,099, 1993.